ANISOTROPY OF STRENGTH IN SINGLE CRYSTALS UNDER PLANE STRAIN COMPRESSION*

G. Y. CHIN,† E. A. NESBITT† and A. J. WILLIAMS†

The strength of a crystal undergoing deformation depends on the crystal orientation and the geometry of deformation. In this paper, the Bishop and Hill analysis (*Phil. Mag.* **42,** pp. 414–427 and pp. 1298–1307 (1957)) is utilized to calculate the stress requirements for f.c.c. crystals of several orientations undergoing plane strain deformation. The latter is frequently found in plastic working operations such as rolling, deep drawing, and wire flattening. Compression tests were conducted on Permalloy (4% Mo–17% Fe–79% Ni) single crystals and on polycrystalline material with the samples confined to a channel to prevent lateral spreading. Strength differences by a factor of two may be obtained this way. The present findings are in good agreement with analysis, although some results are complicated by deformation banding and lattice rotations.

ANISOTROPIE DE RESISTANCE DE MONOCRISTAUX SOUMIS A UNE COMPRESSION EN ETAT PLAN DE DEFORMATION

La résistance d'un cristal soumis à une déformation dépend de l'orientation de ce cristal et de la géométrie de la déformation. Dans cet article, les auteurs utilisent l'analyse de Bishop et Hill (*Phil. Mag.* **42,** pp. 414–427 et pp. 1298–1307 (1957)) pour calculer les conditions de contraintes relatives à des cristaux c.f.c. de différentes orientations soumis à une déformation en état plan de déformation. Ce type de déformation se rencontre en effet dans de nombreuses opérations de déformation plastique, telles que le laminage et l'emboutissage. Les essais de compression ont été exécutés sur des monocristaux de Permalloy (4%Mo–17%Fe–79%Ni); ainsi que sur des échantillons polycristallins, les éprouvettes étant sollicitées à l'aide d'un équipement destiné à empêcher toute expansion latérale. On peut obtenir de cette manière des différences de résistance variant du simple au double. Les résultats des essais sont en bon accord avec l'analyse théorique, bien que certains résultats se compliquent par l'apparition de bandes de déformation et par la rotation du réseau.

DIE ANISOTROPIE DER FESTIGKEIT VON EINKRISTALLEN BEI KOMPRESSION MIT EBENER VERZERRUNG

Die Festigkeit eines plastisch verformten Kristalles hängt von der Kristallorientierung und von der Verformungsgeometrie ab. In dieser Arbeit wird mit Hilfe der Analyse von Bishop und Hill (*Phil. Mag.* **42,** S. 414–427 und S. 1298–1307 (1957)) die erforderliche Spannung für die Verformung mit ebener Verzerrung von k.f.z. Kristallen verschiedener Orientierung berechnet. Diese Verformungsart liegt häufig vor beim Walzen, Ziehen und Drahtabflachen. Kompressionsversuche wurden an Permalloy (4% Mo–17% Fe–79% Ni) Einkristallen durchgeführt, sowie an polykristallinem Material, wobei die Probe zur Vermeidung einer seitlichen Ausbreitung in einen Kanal gebettet wurde. Auf diese Weise kann man Festigkeitsunterschiede bis zu einem Faktor 2 erzielen. Die Ergebnisse sind in guter Ubereinstimmung mit der Analyse, obwohl einige Beobachtungen verwickelter werden durch Bandbildung bei der Verformung und durch Gitterdrehungen.

Since plastic deformation is generally accomplished by a slip or twinning process, the stresses required to deform a crystal will vary with crystal orientation and geometry of deformation. The exploitation of crystallographic texture in strengthening materials—"texture hardening"[1]—has been the subject of several recent investigations.[1–3] Of particular interest is the work of Hosford and Backofen,[3] who applied the Bishop and Hill analysis of slip[4] in calculating the yield strength of textured sheets. The latter method is a simplication of the earlier Taylor[5] analysis and places it on a theoretically sounder basis.

To date the only direct investigation of the basic theory using single crystals has been the work of Hosford,[6] who imposed axial symmetric flow in aluminum crystals by wire drawing. He found a reasonable correlation of the drawing stress with axial orientation as predicted by theory. It appears that additional experiments based on other types of imposed flow are desirable as a further test to the theory. Accordingly, the Bishop and Hill analysis is applied to calculating the compression strength of crystals undergoing plane strain deformation. This type of deformation occurs frequently in plastic working operations such as rolling, deep drawing, and roll-flattening and flat-drawing of fine wires. The latter two processes are important in the manufacture of magnetic tapes for memory device applications. In the present experiment, the analytical results were tested with single crystals of Permalloy (4% Mo–17% Fe–79% Ni) in a specially designed compression apparatus. The results are in general agreement with theory. It is observed that for a given thickness reduction, the strength can vary by a factor of two even in these f.c.c. crystals.

A similar study has been made recently by Hosford[7]

on aluminum crystals. He used an indentation method of approximating plane strain. Good agreement between theory and experiment was likewise obtained.

THE BISHOP AND HILL ANALYSIS

The amount of plastic work per unit volume done by a tensile (or compressive) stress σ_{xx} in the x-direction is

$$dw = \sigma_{xx}d\varepsilon_{xx}, \tag{1}$$

where $d\varepsilon_{xx}$ is the incremental strain in the x-direction. This external work may be equated with that due to shear in the active slip systems,

$$dw = \tau\Sigma d\gamma_i, \tag{2}$$

where τ is the shear stress for slip and is assumed to be equal for all slip systems, and $d\gamma_i$ is the incremental shear for the ith slip system. Equating (1) and (2) yields

$$M = \frac{\sigma_{xx}}{\tau} = \frac{\Sigma d\gamma_i}{d\varepsilon_{xx}} = \frac{dw}{\tau d\varepsilon_{xx}}. \tag{3}$$

As pointed out by Hosford,[3] M is a generalized Schmid factor relating the applied stress for flow to the basic shear stress for slip. It is purely dependent on orientation and on the imposed shape change. Thus, once the latter is fixed (such as plane strain), the value M will vary with orientation alone.

To obtain the appropriate value of M, Bishop and Hill applied the principle of maximum work.* In this method it is noted that an arbitrary strain generally requires five or more independent active slip systems. Since the shear stress for slip is assumed equal for all slip systems, only a limited number of stress states is capable of activating the same shear stress on the five or more slip systems. This number is twenty-eight for cubic metals which slip on $\{111\}\langle110\rangle$ slip systems. According to the principle of maximum work, the appropriate stress state(s) is one in which the work dw of equation (3) is a maximum.

The twenty-eight stress states are reproduced in Table 1. Since these states consists of simple combinations of only six stress terms.

$$A = \sigma_{22} - \sigma_{33}, \quad B = \sigma_{33} - \sigma_{11}, \quad C = \sigma_{11} - \sigma_{22},$$
$$F = \sigma_{23}, \qquad G = \sigma_{31}, \qquad H = \sigma_{12},$$

---

* Equation (3) may be rewritten as

$$\tau = \frac{1}{M}\frac{dw}{d\varepsilon_{xx}} = \frac{dw}{\Sigma d\gamma_i}.$$

For slip to occur, the shear stress τ must be raised to the critical value for slip. This may be done either by minimizing the amount of crystallographic shear $\Sigma d\gamma_i$ (Taylor's minimum shear principle), or by maximizing the amount of plastic work dw (Bishop and Hill's maximum work principle). Both methods give equivalent results, although the latter is generally simpler to apply.

TABLE 1. The 28 stress states of Bishop and Hill*

No.	A	B	C	F	G	H
1	1	-1	0	0	0	0
2	0	1	-1	0	0	0
3	-1	0	1	0	0	0
4	0	0	0	1	0	0
5	0	0	0	0	1	0
6	0	0	0	0	0	1
7	$\frac{1}{2}$	-1	$\frac{1}{2}$	0	$\frac{1}{2}$	0
8	$\frac{1}{2}$	-1	$\frac{1}{2}$	0	$-\frac{1}{2}$	0
9	-1	$\frac{1}{2}$	$\frac{1}{2}$	$\frac{1}{2}$	0	0
10	-1	$\frac{1}{2}$	$\frac{1}{2}$	$-\frac{1}{2}$	0	0
11	$\frac{1}{2}$	$\frac{1}{2}$	-1	0	0	$\frac{1}{2}$
12	$\frac{1}{2}$	$\frac{1}{2}$	-1	0	0	$-\frac{1}{2}$
13	$\frac{1}{2}$	0	$-\frac{1}{2}$	$\frac{1}{2}$	0	$\frac{1}{2}$
14	$\frac{1}{2}$	0	$-\frac{1}{2}$	$-\frac{1}{2}$	0	$\frac{1}{2}$
15	$\frac{1}{2}$	0	$-\frac{1}{2}$	$\frac{1}{2}$	0	$-\frac{1}{2}$
16	$\frac{1}{2}$	0	$-\frac{1}{2}$	$-\frac{1}{2}$	0	$-\frac{1}{2}$
17	0	$-\frac{1}{2}$	$\frac{1}{2}$	0	$\frac{1}{2}$	$\frac{1}{2}$
18	0	$-\frac{1}{2}$	$\frac{1}{2}$	0	$-\frac{1}{2}$	$\frac{1}{2}$
19	0	$-\frac{1}{2}$	$\frac{1}{2}$	0	$\frac{1}{2}$	$-\frac{1}{2}$
20	0	$-\frac{1}{2}$	$\frac{1}{2}$	0	$-\frac{1}{2}$	$-\frac{1}{2}$
21	$-\frac{1}{2}$	$\frac{1}{2}$	0	$\frac{1}{2}$	$\frac{1}{2}$	0
22	$-\frac{1}{2}$	$\frac{1}{2}$	0	$-\frac{1}{2}$	$\frac{1}{2}$	0
23	$-\frac{1}{2}$	$\frac{1}{2}$	0	$\frac{1}{2}$	$-\frac{1}{2}$	0
24	$-\frac{1}{2}$	$\frac{1}{2}$	0	$-\frac{1}{2}$	$-\frac{1}{2}$	0
25	0	0	0	$\frac{1}{2}$	$\frac{1}{2}$	$-\frac{1}{2}$
26	0	0	0	$\frac{1}{2}$	$-\frac{1}{2}$	$\frac{1}{2}$
27	0	0	0	$-\frac{1}{2}$	$\frac{1}{2}$	$\frac{1}{2}$
28	0	0	0	$\frac{1}{2}$	$\frac{1}{2}$	$\frac{1}{2}$

* From J. F. W. Bishop, *Phil. Mag.* **44**, pp. 51–64 (1953).

when referred to cubic axes, the work dw is conveniently expanded as a sum of products of stress and strain with respect to these axes. Thus

$$\begin{aligned} dw &= \sigma_{11}d\varepsilon_{11} + \sigma_{22}d\varepsilon_{22} + \sigma_{33}d\varepsilon_{33} + 2\sigma_{23}d\varepsilon_{23} \\ &\quad + 2\sigma_{31}d\varepsilon_{31} + 2\sigma_{12}d\varepsilon_{21} \\ &= (\sigma_{11} - \sigma_{33})d\varepsilon_{11} + (\sigma_{22} - \sigma_{33})d\varepsilon_{22} + 2\sigma_{23}d\varepsilon_{23} \\ &\quad + 2\sigma_{31}d\varepsilon_{31} + 2\sigma_{12}d\varepsilon_{12}, \end{aligned} \tag{4}$$

by noting that $d\varepsilon_{11} + d\varepsilon_{22} + d\varepsilon_{33} = 0$. Substitution of A, B, etc. into (4) and then inserting into (3) yield

$$\begin{aligned} M = \frac{1}{\tau d\varepsilon_{xx}} [&-Bd\varepsilon_{11} + Ad\varepsilon_{22} + 2Fd\varepsilon_{23} + 2Gd\varepsilon_{31} \\ &+ 2Hd\varepsilon_{12}]. \end{aligned} \tag{5}$$

For the case of plane strain compression under study, let x be the compression axis and z the elongation direction, we have

$$d\varepsilon_{yy} = 0, \quad d\varepsilon_{zz} = -d\varepsilon_{xx}, \quad d\varepsilon_{yz} = d\varepsilon_{zx} = d\varepsilon_{xy} = 0.\dagger \tag{6}$$

---

† Strictly speaking, plane strain does not require that $d\varepsilon_{zx}$ be zero. The latter is usually the case in rolling a polycrystalline sample and is thus a useful simplification in extending the analysis beyond single crystals. It will be seen later that the present test setup does not restrict $d\varepsilon_{yz}$ and $d\varepsilon_{zx}$ to zero, although the symmetry of the operating slip systems in most orientations under study automatically leads to such a zero value.
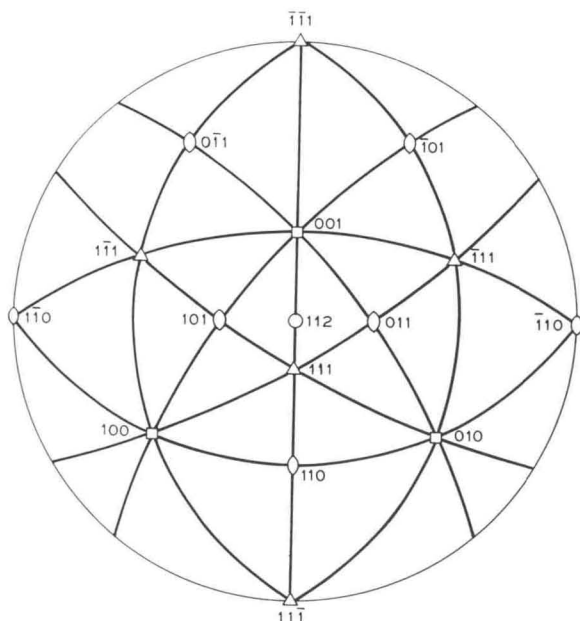
FIG. 1. Standard (112) stereographic projection for a cubic crystal.

Given a crystal orientation, the strain components along the cubic axes ($d\varepsilon_{11}$, etc.) can be found in terms of $d\varepsilon_{xx}$ by using equation (6) and the proper matrix for transforming coordinate axes. The appropriate combination(s) of A, B, etc. can be then be found from among the 28 stress states to maximize the right side of equation (5).

APPLICATION TO F.C.C. METALS

Equation (5) will now be applied to crystals of several highly symmetrical orientations. Because of their symmetry, these orientations are of interest in connection with texture formation and magnetic anisotropy[8] as well as strength considerations. As usual, $\{111\}\langle110\rangle$ slip is assumed.

1. Compression plane (112); elongation direction [$\bar{1}\bar{1}1$].

Let the specimen coordinate axes be $x-[112]$, $y-[1\bar{1}0]$, and $z-[\bar{1}\bar{1}1]$, Fig. 1. The matrix of transformation to the cubic axes (1—[100], 2—[010], 3—[001]) is

	x	y	z
1	$\dfrac{1}{\sqrt{6}}$	$-\dfrac{1}{\sqrt{2}}$	$-\dfrac{1}{\sqrt{3}}$
2	$\dfrac{1}{\sqrt{6}}$	$\dfrac{1}{\sqrt{2}}$	$-\dfrac{1}{\sqrt{3}}$
3	$\dfrac{2}{\sqrt{6}}$	0	$\dfrac{1}{\sqrt{3}}$

Hence, from equation (6) and the transformation matrix, we find that

$$d\varepsilon_{11} = -d\varepsilon_{xx}/6, \quad d\varepsilon_{22} = -d\varepsilon_{xx}/6, \quad d\varepsilon_{33} = d\varepsilon_{xx}/3$$
$$d\varepsilon_{23} = 2d\varepsilon_{xx}/3, \quad d\varepsilon_{31} = 2d\varepsilon_{xx}/3, \quad d\varepsilon_{12} = -d\varepsilon_{xx}/6, \tag{7}$$

and equation (5) becomes

$$M = \frac{1}{\tau}\left[\frac{B}{6} - \frac{A}{6} + \frac{4}{3}F + \frac{4}{3}G - \frac{H}{3}\right]$$
$$= \frac{1}{6\tau}[B - A + 8F + 8G - 2H] \tag{8}$$

By trial, the Bishop and Hill stress states that maximize the right side of equation (8) are Nos. 21 and 25 in Table 1. For No. 21, $A = -\frac{1}{2}$, $B = \frac{1}{2}$, $C = 0$, $F = G = \frac{1}{2}$, $H = 0$; and for No. 25, $A = B = C = 0$, $F = G = \frac{1}{2}$, $H = -\frac{1}{2}$, all multiplied by $\sqrt{6}\,\tau$. We thus have $M = 3\sqrt{6}/2$ in equation (8).

It may be noted that for stress state 21, the active slip systems are $-a_1$, a_2, c_2, $-c_3$, $-d_1$ and d_3 (Bishop and Hill notation, see Appendix 1), while for stress state 25, they are $-a_1$, a_2, c_1, $-c_3$, $-d_2$ and d_3. Since the deformation borders on both stress states, only those slip systems (with proper sign) common to both are activated. This means $-a_1$, a_2, $-c_3$ and d_3.

2. Compression plane (110); elongation direction [$\bar{1}12$].

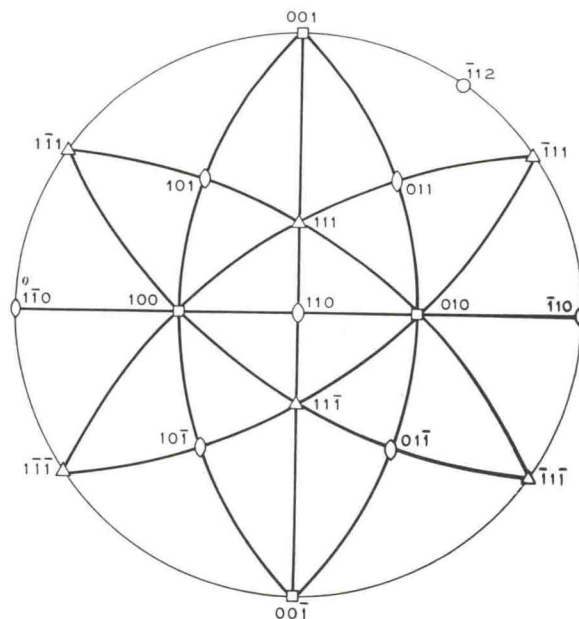Let the specimen axes be $x - [110]$, $y - [\bar{1}1\bar{1}]$ and

FIG. 2. Standard (110) stereographic projection for a cubic crystal.

$z - [\bar{1}12]$, Fig. 2. The matrix for transformation to the cubic axes is

	x	y	z
1	$\dfrac{1}{\sqrt{2}}$	$-\dfrac{1}{\sqrt{3}}$	$-\dfrac{1}{\sqrt{6}}$
2	$\dfrac{1}{\sqrt{2}}$	$\dfrac{1}{\sqrt{3}}$	$\dfrac{1}{\sqrt{6}}$
3	0	$-\dfrac{1}{\sqrt{3}}$	$\dfrac{2}{\sqrt{6}}$

From equation (6) and the transformation matrix, we obtain

$$d\varepsilon_{11} = d\varepsilon_{22} = d\varepsilon_{xx}/3, \; d\varepsilon_{33} = -2d\varepsilon_{xx}/3,$$
$$d\varepsilon_{23} = -d\varepsilon_{xx}/3, \; d\varepsilon_{31} = d\varepsilon_{xx}/3, \; d\varepsilon_{12} = 2d\varepsilon_{xx}/3. \tag{9}$$

Equation (5) becomes

$$M = \frac{1}{\tau}\left[-\frac{B}{3} + \frac{A}{3} - \frac{2F}{3} + \frac{2G}{3} + \frac{4H}{3}\right]$$
$$= \frac{1}{3\tau}\left[-B + A - 2F + 2G + 4H\right]. \tag{10}$$

The Bishop and Hill stress states that maximize the right side of (10) are Nos. 6 and 27, with $M = 4\sqrt{6}/3$.

For stress state 6 ($A = B = C = F = G = 0, H = \sqrt{6}\,\tau$), slip systems $a_1, -a_2, b_1, -b_2, -c_1, c_2, -d_1, d_2$ become active. And for state 27 ($A = B = C = 0, F = -\sqrt{6}\,\tau/2, G = H = \sqrt{6}\,\tau/2$), $-a_2, a_3, b_1, -b_3, -d_1$ and d_2 become active. Hence, the actual operating systems (which are common to both states) are $-a_2, b_1, -d_1$ and d_2. It may be noted that systems $-d_1$ and d_2 are in cross-slip relationship with b_1 and $-a_2$, respectively.

A closer examination of this orientation, however, reveals the possibility of slip on systems $-a_2$ and b_1 alone. It may be shown that under these conditions,

$$d\varepsilon_{xx} = -\frac{2}{\sqrt{6}}\,d\gamma, \quad d\varepsilon_{yy} = 0, \quad d\varepsilon_{zz} = \frac{2}{\sqrt{6}}\,d\gamma,$$
$$d\varepsilon_{yz} = -\frac{\sqrt{3}}{6}\,d\gamma, \quad d\varepsilon_{zx} = 0, \quad d\varepsilon_{xy} = 0, \tag{11}$$

where $d\gamma$ is the incremental shear each on slip systems $-a_2$ and b_1. The only difference between equations (11) and (6) is in the shear strain term $d\varepsilon_{yz}$. However, since the present setup does not restrict $d\varepsilon_{yz}$ to zero, the deformation is expected to occur on $-a_2$ and b_1 alone *if* the total amount of shear $\Sigma|d\gamma_i|$ is less than that for the four slip systems case (Taylor's minimum shear principle). For slip on $-a_2$ and b_1, we have from equation (11),

$$\Sigma\,|d\gamma_i| = 2\,|d\gamma| = \sqrt{6}\,d\varepsilon_{xx}, \tag{12}$$

and for slip on $-a_2, b_1, -d_1$ and d_2,

$$\Sigma\,|d\gamma_i| = Md\varepsilon_{xx} = \frac{4}{3}\sqrt{6}\,d\varepsilon_{xx}, \tag{13}$$

The former value is one-third less and hence we may expect slip on $-a_2$ and b_1 alone.

Similar calculations were carried out for five other orientations of interest. The results for all seven orientations are summarized in Table 2, together with those for the polycrystalline samples. Interestingly, the same operating slip systems as those listed in Table 2 were found earlier by a less rigorous method.[8] As for the polycrystalline material, a value of $M = 1.44\sqrt{6}$ was used. It was derived by Hosford and Backofen[3] from the von Mises yield criterion and the use of Taylor's factor of 3.06 for relating the tensile yield stress to the resolved shear stress for slip in a randomly oriented polycrystalline sample. Although the derivation was based on tensile testing under plane strain conditions, it may be shown that this value is

TABLE 2. Summary of analysis

Sample no.	Compression plane	Elongation direction	M	Slip systems selected	Equation (6) satisfied?
1	112	$\bar{1}\bar{1}1$	$3\sqrt{6}/2$	$-a_1, a_2, -c_3, d_3$	yes
2	110	$\bar{1}12$	$\sqrt{6}$	$-a_2, b_1$	no
			$4\sqrt{6}/3$	$-a_2, b_1, -d_1, d_2$	yes
3	110	001	$\sqrt{6}$	$a_1, -a_2, b_1, -b_2$	yes
4	110	$\bar{1}10$	$2\sqrt{6}$	$-a_1, a_2, -b_1, b_2,$ $c_1, -c_2, d_1, -d_2$	yes
5	001	$\bar{1}00$	$\sqrt{6}$	a_2, b_2, c_2, d_2	yes
6	001	$\bar{1}10$	$\sqrt{6}$	$-c_1, c_2, -d_1, d_2$	yes
7	111	$\bar{1}\bar{1}2$	$3\sqrt{6}/2$	$-b_1, b_2, c_3, -d_3$	yes
8	polycrystal	#1	$1.44\sqrt{6}$	—	yes
9	polycrystal	#2	$1.44\sqrt{6}$	—	yes

Composition of all samples: 4% Mo– 17% Fe– 79% Ni by weight. Samples 8 and 9 were slowly cooled and quenched, respectively, after annealing at 1000°C; grain diameter ~0.04 mm.
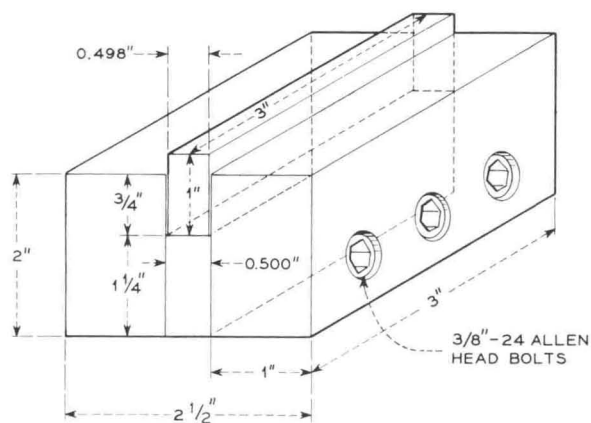
FIG. 3. Compression device for approximating plane strain deformation.

equally applicable in the present case of plane strain compression.

Table 2 indicates that the M values vary by as much as a factor or two. Hence, the theoretical results may be readily tested.

EXPERIMENTAL

A special compression die, somewhat similar to that described by Wever and Schmid,[9] was constructed for quantitative testing of the theory. As illustrated in Fig. 3, the die consists of a hardened steel plunger fitted in the slot of a three-piece assembly, which is secured by bolts to facilitate specimen removal after the test. The specimen, carefully machined to the slot width, is placed between the plunger and the platen. The ensemble is then attached to a Baldwin hydraulic testing machine for compression testing.

This test setup has several advantages in controlling the deformation process. First, the fixed slot width insures negligible lateral spread of the crystal during compression. Secondly, the present setup permits highly accurate orientation alignment even for very small crystals. Finally, this method allows a continuous recording of load versus deflection, an important feature for quantitative stress comparisons. In the present setup, however, there is no constraint on $d\varepsilon_{yz}$ and $d\varepsilon_{zx}$.

The single crystal specimens with orientations listed in Table 2 were machined from large grains which were solidified slowly from the melt. Two fine grained (dia. ~0.04 mm) polycrystalline samples were also tested. Orientation of the single crystals was controlled to about one degree in the finished crystals. Typical dimensions are 0.4 in. long by 0.5 in. wide 0.1 in. thick. After machining, the specimens were etched in *aquaregia* and then electropolished in a solution of CrO_3 and H_3PO_4 to allow slip line observations as well as to reduce friction. Teflon strips 5 mils thick were used as lubricant. Breakdown of these strips (usually in the periphery region in the elongation direction) occurred between twenty and forty per cent thickness reduction depending on the flow characteristics of the sample. Loading rate was equivalent to about 0·01 in/min.

RESULTS AND DISCUSSION

Figure 4 shows typical curves of true compression stress (load divided by instantaneous area) versus true strain (log [initial height/instantaneous height]). The break in the curves is due to temporary unloading to insert new teflon strips. The lower flow stress upon reloading is the result of reduced friction. There is little doubt that the stress measurements were complicated by friction, see Appendix II. However, the friction ought not to vary widely from crystal to crystal. Unloading curves such as those in Fig. 4 indicate that the extra friction stress (above that of a freshly lubricated surface) amounts to about 20%, mainly as a result of some teflon breakdown. Finally, the stress levels reached in the present study are comparable to those under tension (where friction is absent) of a 78% Ni–22% Fe alloy as studied by Vidoz *et al.*[10]
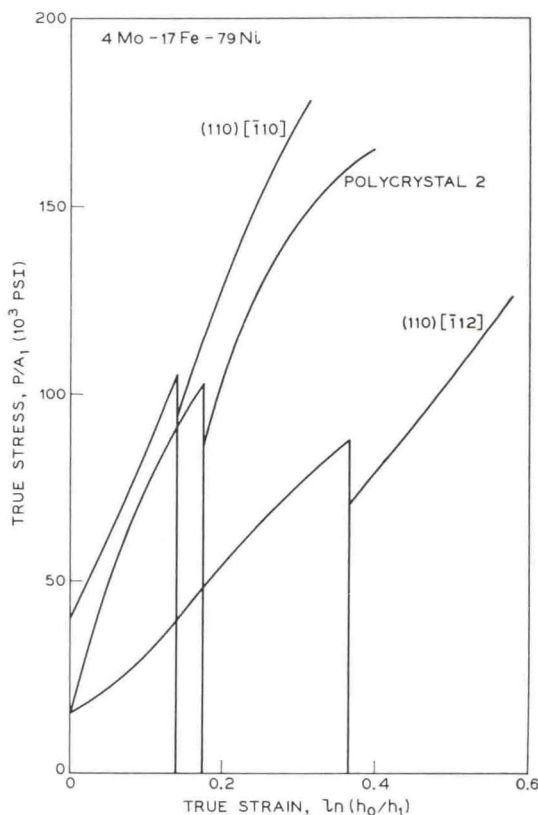

FIG. 4. True compression stress–true thickness strain curves for three samples. 4–79 Mo-Permalloy. Break in curves due to unloading to renew teflon lubricant.
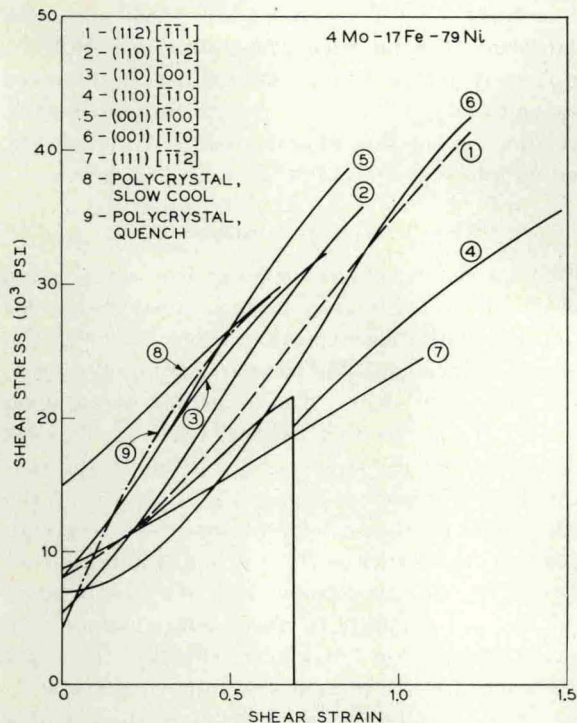
FIG. 5. Resolved shear stress–resolved shear strain curves of all samples tested. 4–79 Mo-Permalloy.

with their difference in M values. For a more quantitative comparison, all curves should be plotted on a resolved shear stress (τ)–resolved shear strain (γ) basis. This is shown in Fig. 5 for all samples, with calculations based on the formulas $\tau = \sigma/M$, $\gamma = M\varepsilon$. If the Bishop and Hill theory is correct, all curves should fall into one.

The majority of the curves do not in fact fall into a band with maximum deviation of $\pm 20\ \%$ from the average. This scatter is within the range of expectations when frictional variation and other inherent errors are considered. Some remarks, however, may be made with several of the samples. First, at large strains crystals 4 and 7 seem to harden less than the average. Examination of crystal 4, which is a $(110)[\bar{1}10]$ orientation, reveals the presence of large deformation bands, Fig. 6. This deviation from homogeneous deformation is expected to result in softening, effectively lowering the M value.[6] On the other hand, for this orientation in aluminum, Hosford[7] has found only slight asterism in the Laue spots. In addition, the τ–γ curve does not deviate from those of the other orientations. Such observations suggest that deformation banding may be absent in aluminum of the $(110)[\bar{1}10]$ orientation. Accordingly, we deformed such a crystal in our apparatus. As Fig. 7 shows, deformation banding was indeed absent. Except for a few long slip lines which appeared very early in the test, only a clothlike mixture of fine slip was found distributed uniformly throughout the surface.
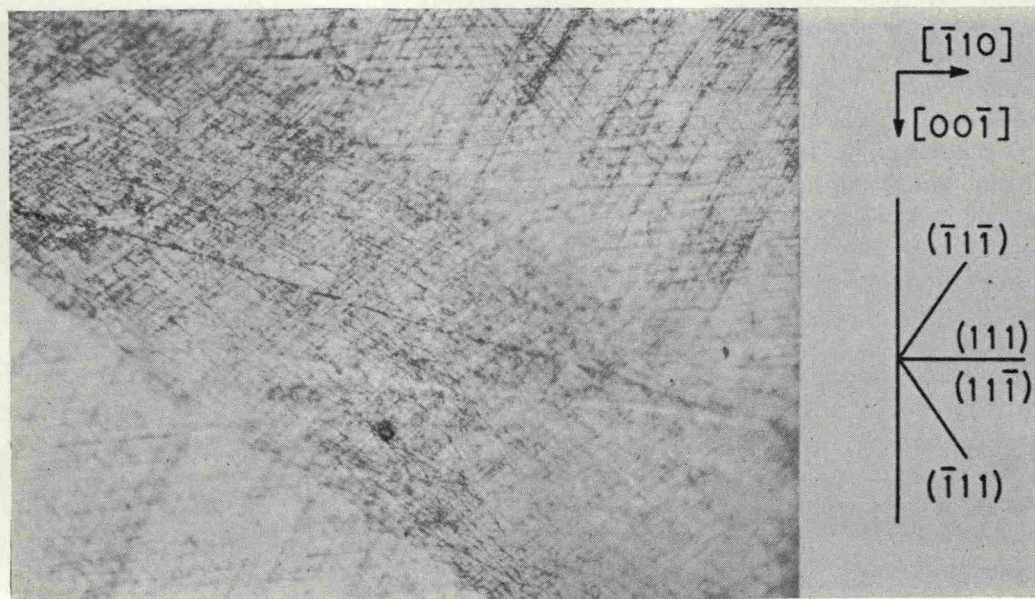
Thus, the relative stress levels among samples, for a given moderate reduction, are thought to reflect mainly the orientation difference as analyzed.

It may be observed in Fig. 4 that the strength of the $(110)[\bar{1}10]$ crystal exceeds that of the $(110)[\bar{1}12]$ crystal by a factor of about 2. This is in qualitative agreement

FIG. 6. Slip traces on top surface of (110) $[\bar{1}10]$ Permalloy crystal after 21.7 % thickness reduction, showing presence of deformation bands. The $[\bar{1}10]$ direction is nearly horizontal. Slip plane traces are noted in margin. $\times$ 280

FIG. 7. Top surface of (110) [Ī10] aluminum crystal after 24% thickness reduction, showing absence of deformation bands. Slip plane traces are noted in margin. × 280

With regard to crystal 7, (111)[ĪĪ2], the lower hardening may result from lattice reorientation, again lowering the M value. Brick and Williamson[11] have found that a (111)[ĪĪ2] brass crystal rotates to a (110)[001] position after an 80% reduction by rolling. It may be noted that $M = \sqrt{6}$ for (110)[001], which is smaller that the value of $M = 3\sqrt{6}/2$ for (111)[ĪĪ2]. Hence if lattice rotation did not occur in the present (111)[ĪĪ2] sample, use of a smaller value of M would

have raised its τ–γ curve in Fig. 5. Using hardness measurements, Brick and Williamson[11] also noted a softening in their (111)[ĪĪ2] brass crystal.

Secondly, the two polycrystalline samples, 8 and 9, fall within the single crystal group. However, they do lie near the top of the list, suggesting a grain size strengthening effect not accounted for in the basic theory. (If a value of $M = 1.35\sqrt{6}$ as derived by Bishop and Hill[4] is used (see Ref. 7) instead of

FIG. 8. Top surface of (110)[Ī12] Permalloy crystal after 50.5% thickness reduction, electropolished, and then further deformed lightly. No constraint on ε_{yz}. Slip plane traces consistent with predicted $-a_2$, (111)[10Ī], and b_2, (11Ī)[011] slips. × 140
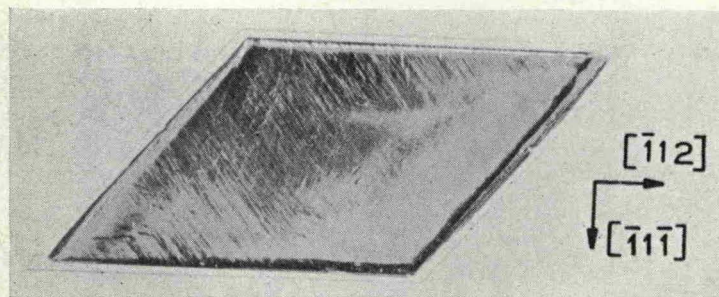
Fig. 9. Top view of (110)[$\bar{1}$12] Permalloy crystal of Fig. 8 after 50.5%
thickness reduction. Transformation of the initially rectangular shape to
a parallelogram indicated presence of ε_{yz}.   × 2.70

$M = 1.44\sqrt{6}$ for the present study, the τ–γ curves would lie higher still. This would accentuate the possible grain size strengthening effect even more.) It may be noted that the difference between samples 8 and 9 in the cooling rate. Sample 8, slowly cooled after a 1000°C anneal, has a much higher yield stress probably as a result of ordering.

Finally, in the case of (110)[$\bar{1}$12] straining (crystal No. 2), a value of $M = \sqrt{6}$ was used in Fig. 5. This corresponds to the two-slip system ($-a_2$ and b_1) operation and leads to the strain equations (11), instead of activating additional slip systems ($-d_1$ and d_2) to conform with equations (6). The two-slip system operation is confirmed by metallographic observation of slip traces on the specimen surface, Fig. 8. In addition, the initially rectangular geometry is changed to a parallelogram after straining, Fig. 9, indicating

the presence of the $d\varepsilon_{yz}$ term (equation (11)) associated with the predicted two-slip system operation. A detailed analysis[12] of the shape change has likewise confirmed that the deformation can be accounted for almost exclusively by the two predicted slip systems $-a_2$ and b_1.

By placing a (110)[$\bar{1}$12] crystal between rectangular polycrystalline blocks during compression, $d\varepsilon_{yz}$ was suppressed. As a result, all four slip systems ($-a_2$, b_1, $-d_1$ and d_2) were found to operate in accordance with analysis, see Fig. 10.

At first glance, the fact that $-d_1$, (1$\bar{1}$1)[011] and d_2, (1$\bar{1}$1)[$\bar{1}$01] can be activated at all seems surprising. The slip plane normal (1$\bar{1}$1) of these two slip systems is perpendicular to the compression axis (see Fig. 2) and hence the resolved shear stress is zero on this basis. In actuality, however, if the shear strain $d\varepsilon_{yz}$ resulting
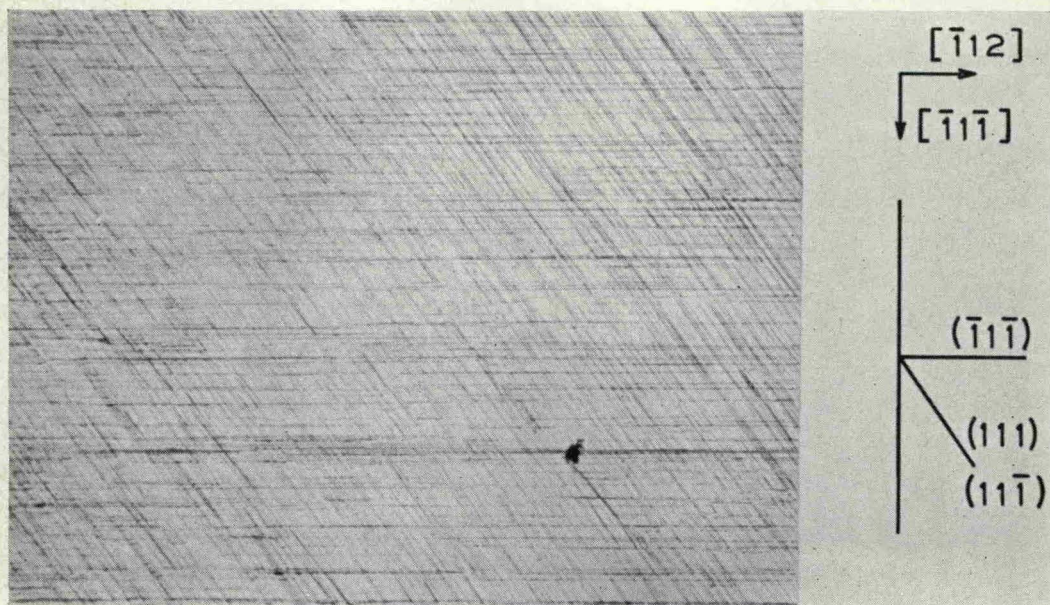

Fig. 10. Top surface of (110)[$\bar{1}$12] Permalloy crystal after 13% thickness reduction. Strain ε_{yz} was suppressed by placing the sample between polycrystalline blocks. Note additional slip traces consistent with predicted new systems $-d_1$, (1$\bar{1}$1)[011] and d_2, (1$\bar{1}$1)[10$\bar{1}$].   × 140

from the operation of $-a_2$, $(111)[10\bar{1}]$ and b_1, $(11\bar{1})[011]$ were suppressed, a shear stress τ_{yz} is generated to activate $-d_1$ and d_2 (in a direction to reduce $d\varepsilon_{yz}$).

CONCLUSIONS

Depending on crystal orientation, the resistance to plane strain deformation can vary by a factor of two even in face-centered cubic material. This resistance arises mainly from the disposition of the slip systems with respect to the deformation geometry. Experiments on Permalloy single crystals confirmed the general validity of a Taylor and Bishop and Hill type analysis. However, we need to take into account such factors as lattice rotations, deformation banding, and relaxation of constraints in the deformation system. The tendencies for lattice rotations and for deformation banding are presumably related in an important way to details of dislocation interactions and would, therefore, depend on such factors as stacking fault energy, testing temperature and strain rates.

ACKNOWLEDGMENTS

REFERENCES

1. W. A. BACKOFEN, W. F. HOSFORD, JR. and J. J. BURKE, *Am. Soc. Metals. Trans. Quart.* **55**, 264 (1962).
2. R. L. WHITELEY and D. E. WISE, *Flat Rolled Products III*, p. 47. Interscience, New York (1962).
3. W. F. HOSFORD, JR. and W. A. BACKOFEN, *Fundamentals of Deformation Processing*, Edited by W. A. BACKOFEN *et al.*, p. 259. Syracuse University Press, Syracuse (1964).
4. J. F. W. BISHOP and R. HILL, *Phil. Mag.* **42**, 414, 1298 (1951).
5. G. I. TAYLOR, *S. Timoshenko 60th Anniversary Volume—Contributions to the Mechanics of Solids*, p. 218. Macmillan, New York (1938).
6. W. F. HOSFORD, JR., *Trans. Met. Soc. AIME* **233**, 329 (1965).
7. W. F. HOSFORD, JR., to be published in *Acta. Met.*
8. G. Y. CHIN, *J. Appl. Phys.* **36**, 2915 (1965).
9. F. WEVER and W. E. SCHMID, *Z. Metallk.* **22**, 133 (1930).
10. A. E. VIDOZ, D. P. LAZAREVIC and R. W. CAHN, *Acta Met.* **11**, 17 (1963).
11. R. M. BRICK and M. A. WILLIAMSON, *Trans. Am. Inst. Min. Metall. Engrs* **143**, 84 (1941).
12. G. Y. CHIN, R. N. THURSTON and E. A. NESBITT, *Trans. Met. Soc. AIME* (1966).
13. E. RABINOWICZ, *Friction and Wear of Materials*, p. 82. Wiley, New York (1965).
14. G. W. PEARSALL and W. A. BACKOFEN, *Trans. Am. Soc. Metal. Engrs* Series B **85**, 329 (1963).
15. *J. Teflon* **5**, 4 (1964).

APPENDIX I

In the Bishop and Hill notation, the following designations are used to represent $\{111\}\langle110\rangle$ slip in f.c.c. metals:

Plane	(111)			$(\bar{1}11)$		
Direction	$01\bar{1}$	$\bar{1}01$	$1\bar{1}0$	$0\bar{1}1$	101	$\bar{1}10$
Shear	a_1	a_2	a_3	b_1	b_2	b_3
Plane	$(\bar{1}11)$			$(1\bar{1}1)$		
Direction	$01\bar{1}$	101	$\bar{1}\bar{1}0$	$0\bar{1}1$	$\bar{1}01$	110
Shear	c_1	c_2	c_3	d_1	d_2	d_3

The shear a_1 represents slip on (111) plane and in the $[01\bar{1}]$ direction in the positive sense. The notation $-a_1$ will be used for either $(\bar{1}\bar{1}\bar{1})[01\bar{1}]$ or $(111)[0\bar{1}1]$ slip, i.e., for shear in the negative sense.

Bishop and Hill have shown that the resolved shear stress on the twelve slip systems, multiplied by $\sqrt{6}$, are equal to:

$$\begin{array}{llll}
\text{for} & a_1, & A - G + H & a_2, \quad B + F - H \\
& b_1, & A + G + H & b_2, \quad B - F - H \\
& c_1, & A + G - H & c_2, \quad B + F + H \\
& d_1, & A - G - H & d_2, \quad B - F + H \\
& & a_3, & C - F + G \\
& & b_3, & C + F - G \\
& & c_3, & C - F - G \qquad\qquad \text{(A1)} \\
& & d_3, & C + F + G,
\end{array}$$

where

$$A = \sigma_{22} - \sigma_{33}, \; B = \sigma_{33} - \sigma_{11}, \; C = \sigma_{11} - \sigma_{22}$$
$$F = \sigma_{23}, \qquad G = \sigma_{31}, \qquad H = \sigma_{12},$$

all referred to the cubic axes.

Once the appropriate stress state from Table 1 is selected according to the maximum work principle, the values A to H are fixed. These values are then entered into equation (A1) to obtain the desired active slip systems. As an example, consider the $(112)[\bar{1}11]$ deformation in the text (case 1). Stress state 21 from Table 1 is one of two states selected. For this state, $A = -\frac{1}{2}$, $B = \frac{1}{2}$, $C = 0$, $F = G = \frac{1}{2}$, $H = 0$, all multiplied by $\sqrt{6}\,\tau$. When these values are entered into equation (A1), the resolved shear stress for slip is reached only in systems $-a_1$, a_2, c_2, $-c_3$, $-d_1$, and d_3. Thus for $-a_1$, $(-A + G - H)/\sqrt{6}\,\tau = 1$, and for b_1, $(A + G + H)/\sqrt{6}\,\tau = 0$ etc.

APPENDIX II

Estimate of friction stress

A simple friction Hill analysis shows that under plane strain compression, the mean compressive stress σ is equal to

$$\bar{\sigma} = \frac{\sigma_y h}{\mu L}\left(e^{\mu L/h} - 1\right), \qquad\qquad \text{(A1)}$$

where σ_y is the yield stress, h is the height, L is the length of the sample, and μ is the coefficient of friction. The value of μ is about 0.04 for teflon.[13] For the present samples, the initial dimensions are $L \approx 0.4$ in., $h \approx 0.1$ in. Hence, $\mu L/h \approx 0.16$ and $\bar{\sigma} \approx 1.08\sigma_y$. The friction contribution thus amounts to about 10% only. After 30% reduction, this contribution is calculated to be about 20%.

If the equation for sliding friction is used,[14]

$$\bar{\sigma}_f = \frac{\tau}{3} \frac{L}{h} \frac{1}{(1-\rho)^{5/2}} \qquad (A2)$$

where $\bar{\sigma}_f$ is the average friction stress, τ is the yield stress in shear for teflon, and ρ is the fractional thickness reduction. For teflon the tensile yield stress is ~ 2000 psi.[15] Hence $\tau = 1000$ psi. Calculations of equation (A2) shows that $\bar{\sigma}_f$ is about 3000 to 7000 psi in the range of 0 to 30% reduction. These values are about 10% of the flow stress of the Permalloy crystals.

The friction on the small side surface is complicated and depends among other factors on the spreading tendency of the crystal. This will contribute further to the scatter in the stress–strain curves.